ACS Chemical Neuroscience

pubs.acs.org/chemneuro Research Article

Destabilized Soluble SOD1 Species as Potential Determinants of Disease Severity in Familial Amyotrophic Lateral Sclerosis

Yoko Hirata,* Yui Kobatake, Hiroko Koyama, Kyoji Furuta, Hiroshi Takemori, and Yuji O Kamatari

Cite This: *ACS Chem. Neurosci.* 2026, 17, 1469−1478 Read Online

ACCESS | Metrics & More | Article Recommendations | Supporting Information

ABSTRACT: Mutations in the Cu/Zn superoxide dismutase (SOD1) gene are linked to familial amyotrophic lateral sclerosis (ALS), yet the identity of the toxic molecular species remains unclear. We investigated the relationship between protein misfolding and pathogenicity by expressing GFP-tagged wild-type and mutant SOD1 (A4V, H46R, G93A) in mouse hippocampal HT22 cells. Western blotting under nonreducing conditions suggested that A4V, associated with rapid disease progression, was largely depleted of properly folded soluble SOD1 and instead produced highly destabilized soluble species. In contrast, H46R, associated with a milder phenotype, showed a moderate reduction in properly folded soluble SOD1 and generated partially folded/native-like conformers. G93A exhibited biochemical characteristics intermediate between those of A4V and H46R. A4V also showed a pronounced loss of GFP fluorescence, indicating severe structural destabilization; the extent of fluorescence loss in A4V, G93A, and H46R broadly correlated with clinical severity. Neither CuATSM nor ebselen—targeting metal binding and disulfide formation, respectively—rescued fluorescence, suggesting broader defects in SOD1 maturation. Nevertheless, both compounds inhibited ferroptosis, a nonapoptotic form of cell death characterized by iron-dependent lipid peroxidation, in HT22 cells, indicating alternative neuroprotective mechanisms. These findings identify destabilized soluble SOD1 species as a key toxic entity in ALS and highlight the utility of GFP-tagged constructs for evaluating folding status and screening therapeutic candidates.

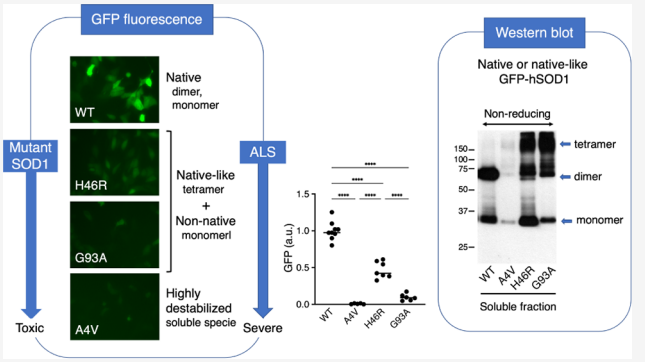

KEYWORDS: *ALS, SOD1, protein misfolding, destabilized soluble SOD1, ferroptosis*

INTRODUCTION

Amyotrophic lateral sclerosis (ALS) is a progressive neurodegenerative disease characterized by the selective loss of motor neurons in the cerebral cortex and spinal cord, leading to severe muscle weakness, paralysis, and ultimately, fatal respiratory failure. In 1993, mutations linked to familial ALS were discovered in the gene encoding Cu/Zn superoxide dismutase (SOD1), which is an antioxidant enzyme that catalyzes the conversion of the superoxide anion to oxygen and hydrogen peroxide.[1] Since then, more than 200 mutations in *SOD1* have been reported in ALS patients (https://alsod.ac.uk/output/gene.php/SOD1), with mutant SOD1 acquiring toxic gain-of-function properties.[2] These mutations are known to disrupt the proper SOD folding by affecting metal binding, intramolecular disulfide bond formation, and dimerization, leading to the accumulation of misfolded protein species.[3,4] Studies utilizing recombinant SOD1 proteins and overexpression systems have demonstrated that these mutations often reduce thermal stability and promote the formation of detergent-insoluble aggregates.[5−7] Furthermore, several studies have employed tagged SOD1 expression in neuronal cell lines and transgenic mouse models to demonstrate that ALS-linked SOD1 mutants readily form aggregates in vivo and in vitro.[8−12] Although large SOD1 aggregates have long been thought to contribute to neurodegeneration, recent evidence suggests that smaller oligomeric species, rather than insoluble aggregates, are the primary neurotoxic entities.[13−15] However, the relationship between the biochemical and biophysical properties of mutant SOD1 and disease severity remain poorly understood.

SOD1-associated familial ALS patients show remarkably broad mean survival times, ranging from approximately 1 to 17 years after diagnosis, depending on the specific mutation.[16,17] In this study, we focused on three of the most common ALS-associated SOD1 mutations: A4V, H46R, and G93A. The A4V mutation, in which alanine is replaced by valine at codon 4, is the most prevalent SOD1 mutation in the United States, accounting for approximately 50% of SOD1-linked ALS cases.

Received: August 21, 2025
Revised: March 23, 2026
Accepted: March 25, 2026
Published: March 27, 2026

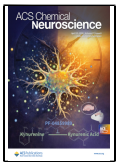

https://doi.org/10.1021/acschemneuro.5c00668
ACS Chem. Neurosci. 2026, 17, 1469−1478

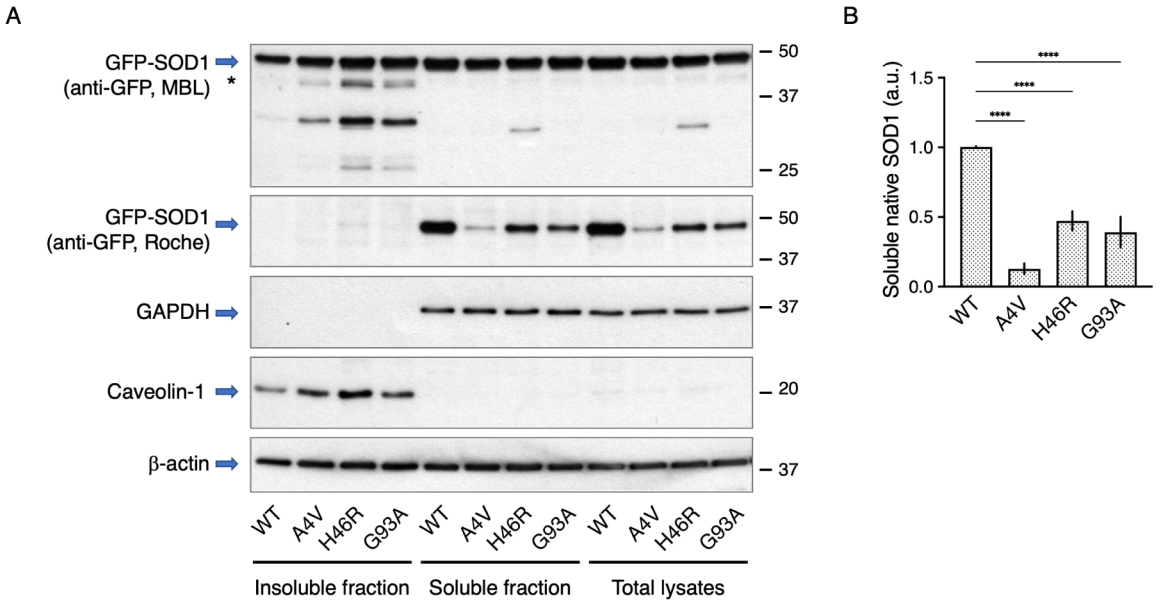

Figure 1. Western blot analysis of overexpressed GFP-SOD1. (A) GFP-SOD1 constructs were transfected into cells for 24 h. Subsequently, Triton X-100-soluble and -insoluble fractions, as well as total cell lysates, were prepared. Samples were separated by SDS-PAGE and subjected to immunoblotting using the indicated antibodies. GAPDH was used as a marker for detergent-soluble proteins, caveolin-1 as a marker for detergent-insoluble proteins, and β-actin as a general loading control. (B) Band intensities of native-like soluble GFP-SOD1 proteins detected with an anti-GFP antibody (Roche) were quantified using ImageJ. Data are presented as relative values normalized to the WT, which was set to 1.0. ****$p < 0.0001$ ($n = 5-8$). Note that the insoluble fraction was adjusted to a buffer volume corresponding to one-tenth of the soluble fraction, based on its total protein content. Therefore, band intensities cannot be directly compared, and the sum of insoluble and soluble fractions does not represent the total lysate.

Clinically, patients with this mutation exhibit significantly shorter disease duration (1.4 ± 0.7 years vs 4.6 ± 6.0 years overall) and faster decline in the ALS Functional Rating Scale-Revised (ALSFRS-R) and forced vital capacity (FVC) compared with non-A4V patients (both $p = 0.02$).[18] The H46R mutation, involving the substitution of histidine with arginine at codon 46, has been reported in Japanese, Pakistani, Chinese, Norwegian, French, and U.S. populations. Although quantitative clinical data on ALSFRS-R or respiratory function are limited, H46R is associated with a much slower disease course, with an average survival of more than 15 years after symptom onset.[19−21] We also examined the G93A mutation (glycine to alanine) due to its widespread use in experimental models. While this mutation is also linked to rapid disease progression, survival times vary depending on clinical care and therapeutic interventions.[22] However, due to the low prevalence of this mutation in ALS patients and the lack of consistent clinical data (e.g., ALSFRS-R scores or FVC decline), conclusions regarding G93A should be interpreted as model-based rather than representative of the broader patient populations.[22,23]

To investigate the misfolding and aggregation behavior of these SOD1 mutants, we employed fusion proteins in which mutant SOD1 was linked to green fluorescent protein (GFP). A similar approach using *Escherichia coli* has been shown to detect protein misfolding based on GFP conformation and fluorescence intensity.[24] In the present study, we expressed SOD1 fusion proteins with an N-terminal GFP-tag and a C-terminal Flag-tag in HT22 mouse hippocampal cells. Protein expression was analyzed by Western blotting using anti-GFP and anti-Flag antibodies, and fluorescence intensity was measured to assess the presence of GFP-tagged SOD1 in live cells.

Our results showed that properly folded soluble SOD1 was nearly undetectable in the A4V mutant and significantly decreased in the H46R and G93A mutants. Moreover, partially folded/native-like conformers were present in the H46R and G93A variants. Notably, the levels of insoluble SOD1 were comparable among all three mutants, suggesting that soluble misfolded species, rather than insoluble aggregates, may play a critical role in determining the clinical severity of ALS. In addition, GFP-SOD1−expressing cells may provide a valuable system for screening candidate molecules that restore proper protein folding by directly targeting misfolded SOD1.

RESULTS

Characterization of GFP-SOD1 Proteins Expressed in Cultured Cells

The expression of GFP-tagged SOD1 (wild type [WT], and A4V, H46R, and G93A variants) was analyzed using monoclonal (Roche) and polyclonal (MBL) anti-GFP, anti-SOD1, and anti-Flag antibodies (Figure 1A, Figure S1). The polyclonal anti-GFP antibody detected GFP-SOD1 in both Triton X-100-soluble and -insoluble fractions, as well as in total cell lysates. Similarly, the anti-Flag and anti-SOD1 antibodies detected the major GFP-SOD1 band along with an additional lower-molecular-weight band (indicated by an asterisk in Figure 1A, Figure S1), confirming that SOD1 was properly tagged with GFP and Flag sequences. Fractionation efficiency was confirmed by GAPDH (soluble marker) and caveolin-1 (insoluble marker).

Notably, the monoclonal anti-GFP antibody (Roche) detected GFP-SOD1 exclusively in the soluble fraction, despite the presence of substantial amounts in the insoluble fraction (see Discussion for details on antibody accessibility). The reduced signal intensity observed for A4V was most

https://doi.org/10.1021/acschemneuro.5c00668
ACS Chem. Neurosci. 2026, 17, 1469−1478

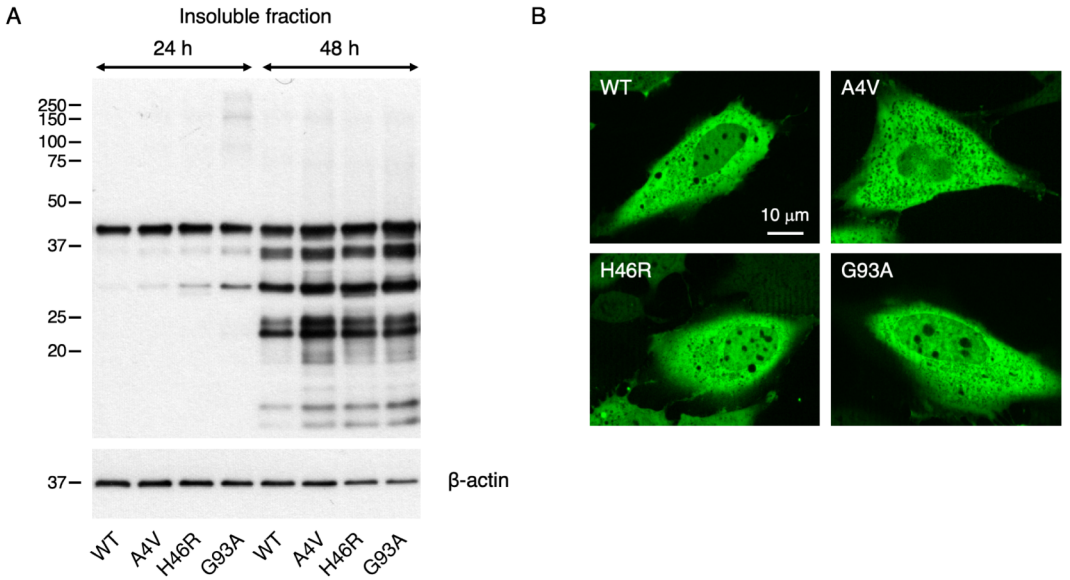

Figure 2. Effect of incubation time on GFP-SOD1 aggregation. (A) Western blot analysis of Triton X-100-insoluble fractions containing overexpressed GFP-SOD1 after 24 and 48 h of incubation. Samples were probed with an anti-GFP (MBL). (B) Fluorescence imaging of GFP-SOD1 in cells transfected for 24 h. Micrographs were acquired as described in Materials and Methods, with exposure times of 0.13 s for WT, 1.2 s for A4V, 0.67 s for H46R, and 0.83 s for G93A. Scale bar, 10 μm.

pronounced, with H46R and G93A showing moderate reductions (Figure 1B), likely reflecting altered GFP conformation within the fusion protein rather than reduced expression of SOD1 itself, as confirmed by other antibodies. In contrast, total GFP-SOD1 levels—as detected by the polyclonal anti-GFP antibody—remained largely unchanged across all variants, with a slight increase in the insoluble fraction of mutant variants compared to WT.

Aggregation of SOD1 Does Not Correlate with ALS Severity

We next investigated whether prolonged incubation influenced aggregation among the SOD1 variants. As SOD1 aggregation is a time-dependent process, an increase in Triton X-100-insoluble protein was expected over time. Indeed, 48 h after transfection, greater amounts of insoluble mutant proteins were observed. However, insoluble protein levels did not differ substantially among the variants (Figure 2A), indicating that the extent of insoluble protein accumulation does not correlate with clinical severity.

To assess intracellular inclusion formation, fluorescence imaging was performed in GFP-SOD1-expressing cells. Consistent with previous findings that SOD1 is widely distributed across the cytosol, mitochondrial intermembrane space, and the nucleus,[25] GFP signals were observed throughout the entire cell. None of the variants exhibited distinct inclusions at 24 h post-transfection (Figure 2B), nor at 48 h (data not shown). This lack of inclusion formation is likely due to relatively low transgene expression levels in the hippocampal HT22 cell line, which may not reach the threshold required for visible inclusions. Thus, the detergent-insoluble fraction observed in our assay likely reflects the accumulation of poorly soluble or misfolded SOD1 species rather than the formation of large visible aggregates.

GFP-SOD1 Mutants Form Noncovalent and Disulfide-Linked Oligomers in the Soluble Fraction under Nonreducing Conditions

To examine oligomer formation, sodium dodecyl sulfate-polyacrylamide gel electrophoresis (SDS-PAGE) followed by Western blotting was performed under nonreducing conditions (i.e., without 2-mercaptoethanol or heat treatment; Figure 3A, right; B, right). With the anti-GFP antibody (Roche), WT displayed two major bands at ~38 kDa and ~75 kDa, likely representing monomeric and dimeric GFP-SOD1, whereas H46R and G93A showed high-molecular-weight species around 150 kDa, suggestive of tetramers. These bands disappeared when iodoacetamide (IAA) was included during lysis (Figure 3A, middle), and under reducing conditions all samples showed only a ~50 kDa monomeric band (Figure 3A, left; B, left), indicating that oligomers were mediated by disulfide bonds formed after cell lysis. Notably, A4V showed only faint signals with anti-GFP (Roche) under both conditions, suggesting severe destabilization or structural alteration.

Using an anti-Flag antibody, two distinct monomeric species were detected under nonreducing conditions: an upper band (monomer-u) predominant in A4V and G93A, and a lower band (monomer-l) more abundant in WT and H46R (Figure 3B, right). These molecular differences imply distinct conformations of folded versus destabilized monomers. However, only upper band was detected under nonreducing conditions when IAA was included during lysis (Figure 3B, middle), suggesting that monomer-u and monomer-l may be SOD1 monomers with the C57−146 disulfide bond reduced and oxidized forms.[26] High-molecular-weight species were also observed in A4V, H46R, and G93A. Interestingly, anti-Flag detected GFP-SOD1 only weakly in WT under nonreducing conditions, but strongly under reducing conditions (Figure 3B, left), suggesting preferential recognition of misfolded conformations that expose the Flag epitope. Collectively, these results indicate that H46R and G93A readily form oligomers, whereas A4V is highly destabilized and poorly recognized by

https://doi.org/10.1021/acschemneuro.5c00668
ACS Chem. Neurosci. 2026, 17, 1469−1478

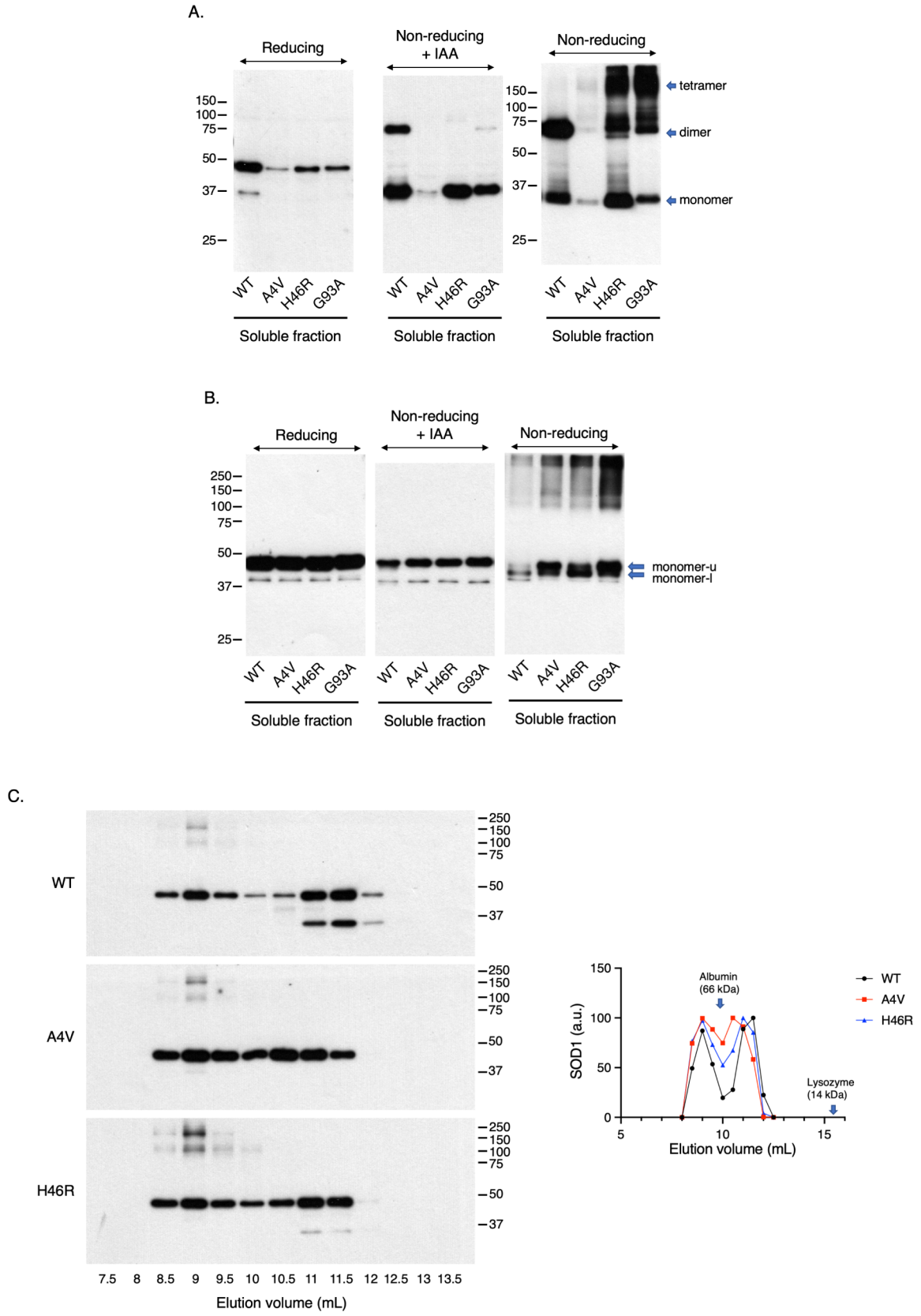

Figure 3. SDS-PAGE/Western blot analysis of Triton X-100-soluble fractions from GFP-SOD1-transfected HT22 cells. Triton X-100-soluble fractions were prepared in the absence (indicated as "Reducing" or "Non-reducing" only) or presence of 20 mM IAA (indicated as "Non-reducing (+IAA)" in the figure). Samples were prepared under reducing and nonreducing conditions (as described in Materials and Methods), separated by SDS-PAGE, and then immunoblotted with anti-GFP (Roche) (A) and anti-Flag (B) antibodies. (C) Size-exclusion chromatography of SOD1-GFP expressed in HT22 cells. The Triton X-100-soluble fraction was subjected to chromatography using a Superdex 75 10/300 GL column (Cytiva).

https://doi.org/10.1021/acschemneuro.5c00668
ACS Chem. Neurosci. 2026, 17, 1469−1478

Figure 3. continued

(Left) Eluted fractions were analyzed by Western blotting using an anti-SOD1 antibody. (Right) Band intensities of SOD1-GFP were quantified using ImageJ, and relative SOD1 levels were plotted.

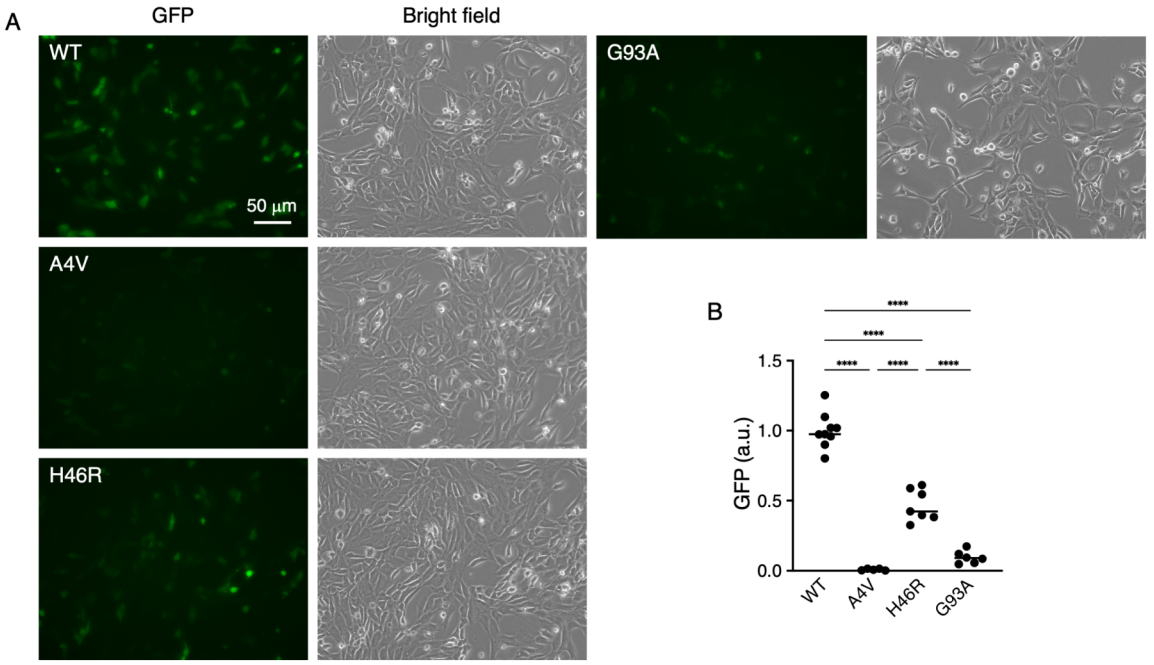

Figure 4. Effect of SOD1 mutations on GFP fluorescence intensity. GFP-SOD1 constructs were transfected for 24 h. (A) Representative fluorescence micrographs are shown. Scale bar, 50 μm. (B) Fluorescence intensity was quantified using a Keyence image measuring system and analysis software (BZ-X Analyzer). ****$p < 0.0001$.

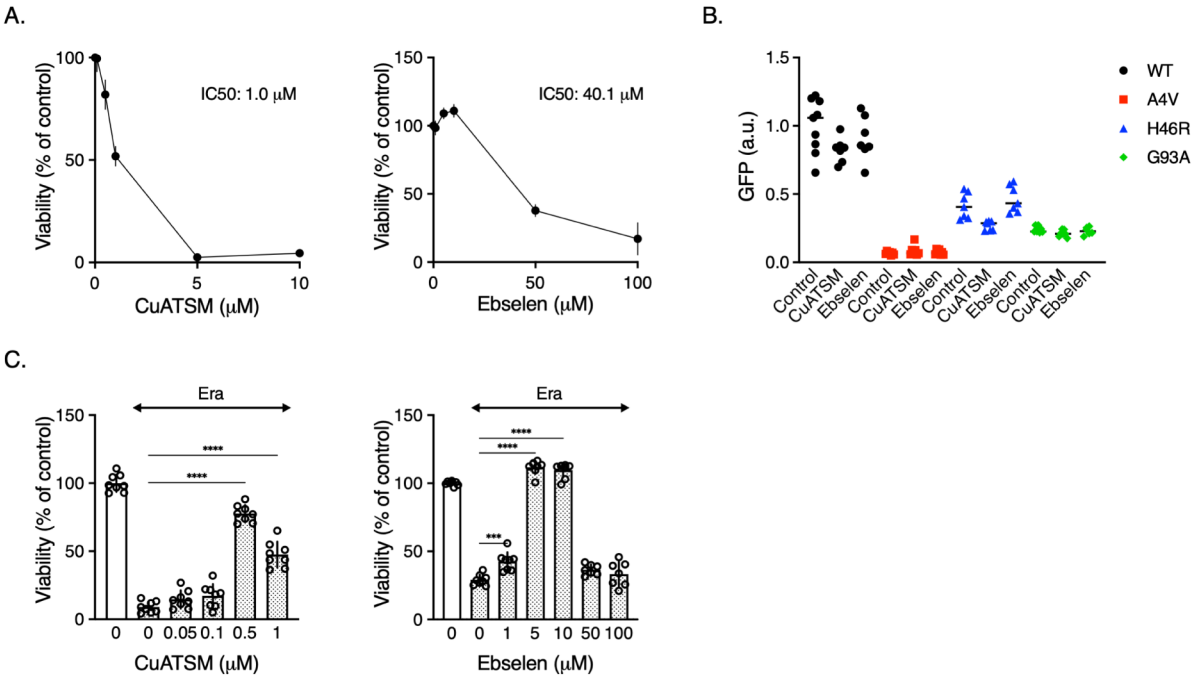

Figure 5. Effect of CuATSM and ebselen on cell viability, GFP fluorescence of mutated SOD1, and erastin-induced ferroptosis in HT22 cells. (A) Cytotoxicity Dose-dependent effects of CuATSM and ebselen on viable HT22 cell number. Cells were incubated with the indicated concentrations of CuATSM and ebselen for 24 h, and cell viability was measured using a WST-8-based cell counting assay. (B) Misfolding The GFP-SOD1 constructs were transfected, and cells were treated as described in Materials and Methods. Fluorescence intensity was quantified using a Keyence image measuring system and analysis software (BZ-X Analyzer). (C) Antiferroptosis Protective effects of 0.5 μM CuATSM and 5 μM ebselen on HT22 cell ferroptosis induced by exposure to 1 μM erastin (Era) for 24 h. Cell viability was measured using a WST-8-based cell counting assay. ***$p < 0.001$; ****$p < 0.0001$.

https://doi.org/10.1021/acschemneuro.5c00668
ACS Chem. Neurosci. 2026, 17, 1469−1478

the Roche anti-GFP antibody. Although the structure of the destabilized soluble species could not be directly assessed, the A4V banding pattern under nonreducing conditions resembled that of G93A, indicating progressive destabilization severity in the order A4V > G93A > H46R.

To further characterize oligomers, size-exclusion chromatography was performed on WT, A4V, and H46R samples prepared in the presence of IAA (Figure 3C). GFP-SOD1 (~43 kDa) eluted in two major peaks: one earlier than albumin (66 kDa) and another between albumin and lysozyme (14 kDa) (Figure 3C, right). The earlier peak likely represents non-disulfide-linked dimers and oligomers that dissociate during SDS-PAGE. Since the Superdex 75 10/300 GL column (Cytiva) is optimized for 3−70 kDa proteins, this peak likely reflects both dimers and higher-order assemblies. These results suggest that alkylation of free sulfhydryls not only blocks the formation of disulfide-mediated oligomers during sample preparation but may also destabilize weaker, noncovalent associations.

Misfolding Decreases GFP Fluorescence Intensity of Mutant SOD1

Because GFP shows fluorescence only upon proper folding, we next evaluated fluorescence intensity in GFP-SOD1-expressing cells. GFP fluorescence became apparent ~24 h post-transfection, and fluorescence intensity was quantified thereafter. Among mutants, fluorescence was lowest in A4V, intermediate in G93A, and highest in H46R (Figure 4), reflecting their relative clinical severity. Western blot analysis confirmed comparable expression levels in WT and mutant-transfected cells (Figure 1), indicating that reduced GFP fluorescence reflects misfolding rather than decreased expression. This interpretation is consistent with results using the conformation-sensitive monoclonal anti-GFP antibody (Roche), further supporting its preferential recognition of properly folded GFP-SOD1. These findings suggest that fluorescence intensity in GFP-SOD1−expressing cells provides a functional readout for misfolding and could serve as a basis for evaluating candidate molecules that stabilize SOD1.

Effect of CuATSM and Ebselen on the GFP Fluorescence Intensity

SOD1 undergoes extensive post-translational modifications, including Zn and Cu binding and disulfide bond formation, to achieve its native dimeric conformation.[4] ALS-associated mutations often disrupt this maturation process. We therefore tested small molecules reported to enhance SOD1 folding using GFP-based misfolding assay (Figure 4). Based on previous findings that copper incorporation may be limiting for SOD1 maturation,[27] we first assessed CuATSM, a copper-delivering compound reported to promote copper loading and ameliorate neurodegeneration in cellular and animal models.[28−30] Cytotoxicity assays (WST-8) indicated that 0.5 μM CuATSM was well tolerated in HT22 cells (Figure 5A), and this concentration was used for subsequent assays. However, CuATSM did not restore GFP fluorescence in A4V, H46R, or G93A mutants (Figure 5B), suggesting that copper supplementation alone is insufficient to correct folding defects.

We next examined ebselen, an organoselenium compound reported to facilitate intramolecular disulfide bond formation.[31] A concentration of 5 μM was selected based on its cytotoxic profile. Similarly to CuATSM, ebselen failed to restore GFP fluorescence in any mutant tested (Figure 5B). These results indicate that neither defective copper binding nor disulfide formation alone is sufficient to restore folding in A4V, H46R, and G93A. It is possible that these mutations disrupt additional aspects of SOD1 maturation, such as monomer folding, dimerization, or chaperone interactions. Although CuATSM and ebselen did not enhance fluorescence in our assay, future studies will be required to directly assess copper incorporation and disulfide bond formation to clarify their roles in SOD1 misfolding.

DISCUSSION

In this study, we utilized GFP-tagged SOD1 fusion proteins to evaluate misfolding based on GFP conformation and fluorescence. Our results showed that A4V primarily formed highly destabilized soluble species in the Triton X-100-soluble fraction, whereas H46R and G93A produced both partially folded monomers and native-like tetramers. In contrast, all mutant variants exhibited similar protein levels in the Triton X-100-insoluble fraction, regardless of clinical severity. These findings suggest that the accumulation of destabilized soluble species—rather than the accumulation of insoluble proteins—may better correlate with disease progression in ALS.

Western blotting with a monoclonal anti-GFP antibody (Roche) supported these observations. The antibody, raised against full-length GFP, efficiently detected soluble WT GFP-SOD1 but showed markedly reduced reactivity toward the insoluble fraction and the A4V and G93A mutants. This suggests that the antibody preferentially recognizes properly folded soluble species, whereas the reduced reactivity toward insoluble fractions and mutant forms is likely due to epitope masking or structural disruption caused by misfolding. However, the Roche monoclonal antibody is directed against GFP rather than SOD1, and the observed differential reactivity may therefore reflect conformational changes within GFP itself or interactions between GFP and the fused SOD1 protein. At the same time, GFP folding and fluorescence are known to be sensitive to the folding state of its fusion partner,[32] supporting the idea that structural perturbations in SOD1 could indirectly influence GFP recognition.

Misfolding and aggregation of disease-related proteins are hallmarks of many neurodegenerative disorders, including ALS and Alzheimer's disease. While insoluble aggregates were long regarded as toxic, increasing evidence indicates that soluble intermediates exert greater pathogenicity. In Alzheimer's disease, for example, soluble Aβ oligomers correlate more strongly with cognitive decline and synaptic dysfunction than insoluble plaques,[33,34] leading to therapeutic strategies that selectively target soluble species. By analogy, our results support the view that soluble misfolded SOD1 species may represent important pathogenic entities in ALS.

Structurally, A4V predominantly formed highly destabilized soluble conformers, whereas H46R and G93A retained partially folded or native-like assemblies. Although oligomer formation was abolished by IAA, size-exclusion chromatography revealed abnormal species eluting at higher molecular weights. One possible interpretation is that these represent noncovalently associated assemblies that are stabilized in the reducing cytosolic environment but become disulfide linked once cells are lysed and exposed to oxidative conditions. However, a similar shift in SEC profiles has previously been attributed to unfolded monomeric SOD1 with an enlarged hydrodynamic radius.[35] Thus, our data may reflect a mixture of unfolded monomers and weakly assembled noncovalent complexes. Further studies will be required to distinguish

https://doi.org/10.1021/acschemneuro.5c00668
ACS Chem. Neurosci. 2026, 17, 1469−1478

between these possibilities and to clarify how oxidative stress influences SOD1 oligomerization in intact cells. In addition, structural characterization of the SEC fractions using spectroscopic approaches such as circular dichroism or infrared spectroscopy may help clarify the conformational differences among SOD1 variants.

The two monomeric bands on SDS-PAGE may represent disulfide-reduced and -oxidized forms,[26] as the variant-specific patterns—A4V and G93A favoring the upper band versus WT largely in the lower band—suggest that loss of the C57-146 disulfide bond destabilizes the monomer. Such destabilized monomers may associate through noncovalent interactions, which could explain why SEC revealed higher-molecular weight elution profiles despite the disappearance of disulfide-linked oligomers in the presence of IAA. Notably, G93A exhibited greater destabilization than H46R in our assay. Taken together, while soluble oligomers may contribute to neurotoxicity, the most pathogenic entities appear to be destabilized soluble species, consistent with the aggressive clinical course of A4V.[17,22] Previous computational studies demonstrated the cytotoxic potential of non-native SOD1 oligomers, including trimers, in motor neuron-like cells.[13−15] Our study provides evidence for native-like soluble tetramers in H46R and G93A, alongside highly destabilized soluble species in A4V, in a cellular model.

The fluorescence data further supported these findings. Similar to a previous study showing that EGFP fluorescence correlates with proper folding of p53 fusion proteins,[24] we observed that SOD1-GFP fluorescence intensity closely reflected folding status, consistent with clinical severity. Zhang and Zhu (2006) likewise reported reduced fluorescence for A4V and G93A SOD1 fusion proteins in cultured cells.[36] Thus, GFP fluorescence provides a reliable marker for SOD1 folding in cellular assays. However, we cannot exclude the possibility that oxidative stress or intracellular pH alterations associated with mutant SOD1 expression may influence GFP fluorescence and potentially affect antibody recognition independently of SOD1 structural destabilization.[37,38]

SOD1 maturation requires metal binding and disulfide formation,[39,40] processes frequently disrupted by ALS mutations. Although copper deficiency has been proposed,[27] Cu-ATSM treatment did not restore fluorescence in our system suggesting that copper deficiency alone may not account for the misfolding of A4V, H46R, or G93A variants under these conditions. Interestingly, the H46R mutant, which disrupts a copper-binding histidine residue, displayed stronger fluorescence than A4V and G93A, implying that factors beyond copper loading—such as global structural destabilization—may contribute to the folding defect. Similarly, ebselen, which promotes disulfide formation, failed to restore fluorescence. While this may reflect limited efficacy under our experimental conditions, the disulfide status of SOD1 was not directly measured, which remains a limitation. Nevertheless, both compounds significantly suppressed ferroptosis in HT22 cells (Figure 5C), consistent with their known antioxidant activities. Recent studies showed that Cu-ATSM possesses radical-trapping antioxidant properties and protects neurons from ferroptosis, an iron-dependent oxidative stress implicated in ALS pathogenesis.[41,42] Likewise, ebselen protected HT22 cells from glutamate-induced oxidative cell death, which shares features with ferroptosis.[43] Collectively, these findings suggest that while promoting proper SOD1 folding remains challenging, the antiferroptotic effects of Cu-ATSM and ebselen may offer therapeutic benefit. Moreover, our cell-based SOD1 expression system provides a useful assay for screening compounds that stabilize SOD1 conformation.

A limitation of this study is that GFP tagging may influence the biophysical properties of SOD1, including its stability, although most SOD1 fusion proteins appear to retain similar stability when expressed in mammalian cells such as PC12.[44] Another challenge is the difficulty in characterizing the conformations of unfolded proteins, which often exist as dynamic random coils of rapidly fluctuating structures. As a result, identifying the specific toxic species responsible for pathogenicity across different SOD1 mutants remains a major obstacle. Future studies employing high-resolution structural techniques such as NMR spectroscopy or cryo-electron microscopy will be necessary to resolve these conformational states.

CONCLUSIONS

Our study demonstrated that the expression patterns of SOD1 mutants in HT22 cells reflect, at least in part, the relative clinical severities reported for these variants in ALS patients. The A4V variant primarily produced highly destabilized soluble monomers and oligomers, whereas H46R and G93A retained both non-native monomers and native-like oligomers, predominantly tetramers. Among the tested variants, A4V-SOD1-GFP showed the greatest reduction in fluorescence, consistent with extensive misfolding (Figure 6). These findings highlight the utility of fluorescence-based assays not only for evaluating SOD1 folding status but also for screening potential therapeutic compounds in ALS.

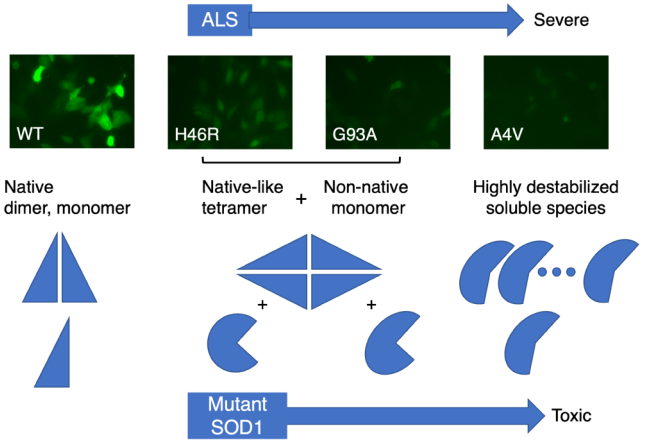

Figure 6. Summary of the formation of native-like and destabilized soluble SOD1 species in ALS-associated SOD1 variants.

MATERIALS AND METHODS

Materials

Pefabloc SC was obtained from Merck (Darmstadt, Germany), collagen Type I (C7661) from Sigma-Aldrich (St. Louis, MO, USA), CuATSM from Cayman Chemical (Ann Arbor, MI, USA), ebselen from Tokyo Chemical Industry (Tokyo, Japan), and erastin from MedChemExpress (Monmouth Junction, NJ, USA).

Plasmid Construction

Human GFP-SOD1-Flag expression plasmids including WT, A4V mutation (in which alanine at codon 4 is replaced by valine), H46R mutation (in which histidine at codon 46 is replaced by arginine), or

https://doi.org/10.1021/acschemneuro.5c00668
ACS Chem. Neurosci. 2026, 17, 1469−1478

G93A mutation (in which glycine at codon 93 is replaced by arginine) were constructed by Genscript Biotechnology (Tokyo, Japan).

Cell Culture

Immortalized hippocampal HT22 cells (RRID: CVCL_0321) were cultured in Dulbecco's modified Eagle's medium (DMEM; Wako Pure Chemicals, Osaka, Japan, Cat# 041-29775) supplemented with 5% fetal bovine serum (FBS; Gibco, Thermo Fisher Scientific, Waltham, MA, USA) at 37 °C in a humidified 5% CO_2 atmosphere. Cells were replaced either at passage 30−40 or every 3 months from the original frozen stocks.

Cell Imaging and Fluorescence Quantification

Cells were seeded at a density of 2×10^5 per 35 mm collagen-coated glass-bottom dish (AGC Techno Glass, Shizuoka, Japan) and cultured in DMEM supplemented with 5% FBS for 1 day. Transfection of SOD1 plasmids (2.5 μg) was then performed using Lipofectamine LTX (Thermo Fisher Scientific) according to the manufacturer's protocol. The medium was changed to standard medium 4 h after transfection and cultured for the specified periods. Fluorescence imaging was performed using a Keyence BZ-X810 microscope (Keyence Corporation, Osaka, Japan), equipped with an optical sectioning algorithm system. Cells were plated in either a 6-well or 12-well plate, and fluorescence intensity was assessed using a digital microscopy (BZ-X810) with subsequent analysis performed via the BZ-X Analyzer software (Keyence Corporation).

Cell Viability Assay

Cell viability based on intracellular dehydrogenase activity was determined with the water-soluble tetrazolium salt (WST-8) using the Cell Counting Kit-8 (Dojindo Laboratories, Kumamoto, Japan, cat# CK04) according to the manufacturer's protocol. HT22 cells (1.2×10^4/well) were plated on 96-well plates and cultured for 1 day. Cells were treated under the specified conditions for 24 h in 200 μL of medium, following which they were incubated with the WST-8 solution for 2 or 3 h at 37 °C. The maximum absorption of the WST-8 formazan at 450 nm was measured with a microplate reader. Cell viability was calculated as the percentage of viable cells relative to that of the untreated controls.

Preparation of Triton X-100-Soluble and -Insoluble Fractions

Cells were grown on 6-well plates (2.4×10^5/well) and transfected with 2.5 μg of SOD1 plasmids using Lipofectamine LTX (Thermo Fisher Scientific), according to the manufacturer's protocol. Four hours after transfection, the culture medium was replaced with standard medium, and cells were incubated for the indicated time periods. Triton X-100-soluble and -insoluble fractions were prepared as previously described, with slight modifications.[45] Briefly, cells were collected and lysed by vortexing in TN-T buffer (50 mM Tris-HCl [pH 7.4], 150 mM NaCl, 1% Triton X-100, 1 mM Pefabloc) and kept on ice for 15 min. IAA was added in TN-T buffer at 20 mM where indicated (e.g., experiments in Figure 3). Lysates were centrifuged at 18,000*g* for 15 min at 4 °C. The supernatant (Triton-soluble fraction) was collected, and the protein concentration was determined using a DC Protein Assay Kit (Bio-Rad Laboratories, Hercules, CA, USA) with bovine serum albumin as the standard. Laemmli sample buffer (62.5 mM Tris-HCl [pH 6.8], 2% SDS, 10% glycerol, 0.025% bromophenol blue) and 5% 2-mercaptoethanol were added to the soluble fraction. The precipitate (Triton-insoluble fraction) was washed twice with TN-T buffer, then resuspended and sonicated in Laemmli sample buffer containing 5% 2-mercaptoethanol. The insoluble fraction was adjusted to a buffer volume corresponding to one-tenth of the soluble fraction, based on its total protein content. For total cell lysates, cell pellets were sonicated in Laemmli sample buffer containing 5% 2-mercaptoethanol. All protein samples were heated at 95−100 °C for 5 min prior to SDS-PAGE.

Western Blotting

Proteins were separated by SDS-PAGE and transferred to Immobilon-P membranes (Merck KGaA, Darmstadt, Germany) with a transfer buffer (20 mM Tris, 150 mM glycine, 20% methanol). To visualize low-abundance proteins in the insoluble fraction, a proportionally larger amount of insoluble protein was loaded, compared to 10 μg of soluble protein and 10 μg of total lysate. Membranes were blocked with 5% nonfat dry milk in phosphate-buffered saline (PBS) containing 0.05% Tween-20 (PBST) for at least 60 min and then incubated overnight at 4 °C with the following primary antibodies: polyclonal anti-GFP (1:1000; Medical & Biological Laboratories (MBL), Tokyo, Japan, RRID:AB_591819), monoclonal anti-GFP (0.5 μg/mL; Roche, RRID:AB_390913), monoclonal anti-Flag M2 (1 μg/mL; Sigma-Aldrich, RRID:AB_262044), monoclonal anticaveolin-1 (0.5 μg/mL; Abcam, Cambridge, UK, RRID:AB_443609), monoclonal anti-SOD1 (0.5 μg/mL; Proteintech, Rosemont, IL, USA, RRID:AB_308477), monoclonal antiglyceraldehyde-3-phosphate dehydrogenase (GAPDH; 0.1 μg/mL; Acris Antibodies, San Diego, CA, USA, RRID:AB_1616730), and polyclonal anti-β-actin (1:1000; MBL, RRID:AB_10598196). After washing three times with PBST (15 min each, with shaking), the membranes were incubated with horseradish peroxidase-conjugated secondary antibodies (1:2000−1:3000; Cell Signaling Technology, Danvers, MA, USA) at 25 °C for 90 min. The membranes were then washed again three times with PBST (15 min each, with shaking), and immunoreactive bands were visualized using either an enhanced chemiluminescence reagent (Cytiva, Tokyo, Japan) or SuperSignal West Dura Extended Duration Substrate (Thermo Fisher Scientific), according to the manufacturers' protocols. Band intensities were quantified using ImageJ software (NIH, Bethesda, MD, USA).

Size-Exclusion Chromatography of Triton X-100-Soluble Fraction

HT22 cells were plated in 25 cm^2 flasks at a density of 1×10^6 cells and transfected with hSOD1-GFP as described above. After harvesting, the Triton X-100-soluble fraction was prepared in the presence of 20 mM IAA and filtered through a 0.22-μm syringe filter. Size-exclusion chromatography was performed using a Superdex 75 10/300 GL column (Cytiva), which provides high resolution for peptides and proteins in the molecular weight range of 3,000−70,000. The column was equilibrated with 0.05 M sodium phosphate buffer (pH 7.3) containing 0.15 M NaCl, and chromatography was carried out at a flow rate of 0.5 mL/min. Fractions of 0.5 mL were collected, and 10-μL aliquots were analyzed by SDS-PAGE under nonreducing conditions followed by Western blotting.

Statistical Analysis

All statistical analyses were conducted using GraphPad Prism 8 (GraphPad Software, San Diego, CA, USA, RRID:SCR_002798). Treatment group means were compared by one-way ANOVA followed by post hoc Dunnett's test if multiple data sets were compared to a control group or Tukey's test in all other cases. *P*-values are noted in the figure legends.

■ ASSOCIATED CONTENT

Supporting Information

The Supporting Information is available free of charge at https://pubs.acs.org/doi/10.1021/acschemneuro.5c00668.

Western blot analysis of overexpressed GFP-SOD1 (PDF)

■ AUTHOR INFORMATION

Corresponding Author

Yoko Hirata − *Life Science Research Center, Institute for Advanced Study, Gifu University, Gifu 501-1193, Japan;* orcid.org/0000-0002-7081-4937; Email: morita.yoko.m1@f.gifu-u.ac.jp

Authors

Yui Kobatake − *Department of Veterinary Medicine, Faculty of Applied Biological Sciences and Center for One Medicine*

https://doi.org/10.1021/acschemneuro.5c00668
ACS Chem. Neurosci. 2026, 17, 1469−1478

Innovative Translational Research, Institute for Advanced Study, Gifu University, Gifu 501-1193, Japan

Hiroko Koyama − *Department of Chemistry and Biomolecular Science, Faculty of Engineering, Graduate School of Natural Science and Technology, and United Graduate School of Drug Discovery and Medical Information Sciences, Gifu University, Gifu 501-1193, Japan*

Kyoji Furuta − *Gifu Exosome Co., Ltd., Gifu 500-8384, Japan*

Hiroshi Takemori − *Department of Chemistry and Biomolecular Science, Faculty of Engineering, Graduate School of Natural Science and Technology, and United Graduate School of Drug Discovery and Medical Information Sciences, Gifu University, Gifu 501-1193, Japan*

Yuji O Kamatari − *Life Science Research Center, Institute for Advanced Study, Gifu University, Gifu 501-1193, Japan; United Graduate School of Drug Discovery and Medical Information Sciences, Institute for Glyco-core Research (iGCORE), and Center for One Medicine Innovative Translational Research, Institute for Advanced Study, Gifu University, Gifu 501-1193, Japan*

Complete contact information is available at: https://pubs.acs.org/10.1021/acschemneuro.5c00668

Author Contributions

Y.H.: conceptualization, funding acquisition, investigation, methodology, supervision, validation, writing—original draft, writing—review and editing. Y.K.: data curation, formal analysis, investigation, methodology. H.K.: resources. K.F.: resources. H.T.: funding acquisition, resources, supervision. Y.O.K.: conceptualization, funding acquisition, project administration, resources.

Notes

The authors declare no competing financial interest.

■ ACKNOWLEDGMENTS

The authors are grateful to the "Tokai National Higher Education and Research System Equipment Sharing System". We appreciate the late Dr. David Schubert for the generous gift of HT22 cells. This work was supported by in part by the Japan Society for the Promotion of Science KAKENHI [grant number JP22K11824, Y.H.], and Japan Agency for Medical Research and Development [grant number JP24ym0126814, Y.O.K.]. The authors would also like to thank Enago (www.enago.com) for English editing.

■ ABBREVIATIONS

ALS, amyotrophic lateral sclerosis; DMEM, Dulbecco's modified Eagle's medium; FBS, fetal bovine serum; GAPDH, glyceraldehyde-3-phosphate dehydrogenase; GFP, green fluorescent protein; IAA, iodoacetamide; PBS, phosphate-buffered saline; SOD, superoxide dismutase; SDS-PAGE, sodium dodecyl sulfate-polyacrylamide gel electrophoresis

■ REFERENCES

(1) Rosen, D. R.; Siddique, T.; Patterson, D.; Figlewicz, D. A.; Sapp, P.; Hentati, A.; Donaldson, D.; Goto, J.; O'Regan, J. P.; Deng, H. X.; et al. Mutations in Cu/Zn superoxide dismutase gene are associated with familial amyotrophic lateral sclerosis. *Nature* **1993**, *362*, 59−62.

(2) Siddique, T.; Deng, H.-X. Genetics of amyotrophic lateral sclerosis. *Hum. Mol. Genet.* **1996**, *5* (Supplement_1), 1465−1470.

(3) Valentine, J. S.; Hart, P. J. Misfolded CuZnSOD and amyotrophic lateral sclerosis. *Proc. Natl. Acad. Sci. U. S. A.* **2003**, *100*, 3617−3622.

(4) McAlary, L.; Yerbury, J. J. Strategies to promote the maturation of ALS-associated SOD1 mutants: small molecules return to the fold. *Neural Regener. Res.* **2019**, *14*, 1511−1512.

(5) Rodriguez, J. A.; Valentine, J. S.; Eggers, D. K.; Roe, J. A.; Tiwari, A.; Brown, R. H., Jr.; Hayward, L. J. Familial amyotrophic lateral sclerosis-associated mutations decrease the thermal stability of distinctly metallated species of human copper/zinc superoxide dismutase. *J. Biol. Chem.* **2002**, *277*, 15932−15937.

(6) Furukawa, Y.; O'Halloran, T. V. Amyotrophic lateral sclerosis mutations have the greatest destabilizing effect on the apo- and reduced form of SOD1, leading to unfolding and oxidative aggregation. *J. Biol. Chem.* **2005**, *280*, 17266−17274.

(7) Prudencio, M.; Hart, P. J.; Borchelt, D. R.; Andersen, P. M. Variation in aggregation propensities among ALS-associated variants of SOD1: correlation to human disease. *Hum. Mol. Genet.* **2009**, *18*, 3217−3226.

(8) Matsumoto, G.; Stojanovic, A.; Holmberg, C. I.; Kim, S.; Morimoto, R. I. Structural properties and neuronal toxicity of amyotrophic lateral sclerosis-associated Cu/Zn superoxide dismutase 1 aggregates. *J. Cell Biol.* **2005**, *171*, 75−85.

(9) Niwa, J.; Yamada, S.; Ishigaki, S.; Sone, J.; Takahashi, M.; Katsuno, M.; Tanaka, F.; Doyu, M.; Sobue, G. Disulfide bond mediates aggregation, toxicity, and ubiquitylation of familial amyotrophic lateral sclerosis-linked mutant SOD1. *J. Biol. Chem.* **2007**, *282*, 28087−28095.

(10) Wang, J.; Farr, G. W.; Zeiss, C. J.; Rodriguez-Gil, D. J.; Wilson, J. H.; Furtak, K.; Rutkowski, D. T.; Kaufman, R. J.; Ruse, C. I.; Yates, J. R., III; et al. Progressive aggregation despite chaperone associations of a mutant SOD1-YFP in transgenic mice that develop ALS. *Proc. Natl. Acad. Sci. U. S. A.* **2009**, *106*, 1392−1397.

(11) Farrawell, N. E.; Lambert-Smith, I.; Mitchell, K.; McKenna, J.; McAlary, L.; Ciryam, P.; Vine, K. L.; Saunders, D. N.; Yerbury, J. J. $SOD1^{A4V}$ aggregation alters ubiquitin homeostasis in a cell model of ALS. *J. Cell Sci.* **2018**, *131*, 209122.

(12) Prudencio, M.; Borchelt, D. R. Superoxide dismutase 1 encoding mutations linked to ALS adopts a spectrum of misfolded states. *Mol. Neurodegener.* **2011**, *6*, 77.

(13) Proctor, E. A.; Fee, L.; Tao, Y.; Redler, R. L.; Fay, J. M.; Zhang, Y.; Lv, Z.; Mercer, I. P.; Deshmukh, M.; Lyubchenko, Y. L.; Dokholyan, N. V. Nonnative SOD1 trimer is toxic to motor neurons in a model of amyotrophic lateral sclerosis. *Proc. Natl. Acad. Sci. U. S. A.* **2016**, *113*, 614−619.

(14) Zhu, C.; Beck, M. V.; Griffith, J. D.; Deshmukh, M.; Dokholyan, N. V. Large SOD1 aggregates, unlike trimeric SOD1, do not impact cell viability in a model of amyotrophic lateral sclerosis. *Proc. Natl. Acad. Sci. U. S. A.* **2018**, *115*, 4661−4665.

(15) Choi, E. S.; Dokholyan, N. V. SOD1 oligomers in amyotrophic lateral sclerosis. *Curr. Opin. Struct. Biol.* **2021**, *66*, 225−230.

(16) Kaur, S. J.; McKeown, S. R.; Rashid, S. Mutant SOD1 mediated pathogenesis of Amyotrophic Lateral Sclerosis. *Gene* **2016**, *577*, 109−118.

(17) Cudkowicz, M. E.; McKenna-Yasek, D.; Sapp, P. E.; Chin, W.; Geller, B.; Hayden, D. L.; Schoenfeld, D. A.; Hosler, B. A.; Horvitz, H. R.; Brown, R. H. Epidemiology of mutations in superoxide dismutase in amyotrophic lateral sclerosis. *Ann. Neurol.* **1997**, *41*, 210−221.

(18) Bali, T.; Self, W.; Liu, J.; Siddique, T.; Wang, L. H.; Bird, T. D.; Ratti, E.; Atassi, N.; Boylan, K. B.; Glass, J. D.; Maragakis, N. J.; Caress, J. B.; McCluskey, L. F.; Appel, S. H.; Wymer, J. P.; Gibson, S.; Zinman, L.; Mozaffar, T.; Callaghan, B.; McVey, A. L.; Jockel-Balsarotti, J.; Allred, P.; Fisher, E. R.; Lopate, G.; Pestronk, A.; Cudkowicz, M. E.; Miller, T. M. Defining SOD1 ALS natural history to guide therapeutic clinical trial design. *J. Neurol., Neurosurg. Psychiatry* **2017**, *88*, 99−105.

(19) Arisato, T.; Okubo, R.; Arata, H.; Abe, K.; Fukada, K.; Sakoda, S.; Shimizu, A.; Qin, X. H.; Izumo, S.; Osame, M.; Nakagawa, M. Clinical and pathological studies of familial amyotrophic lateral

sclerosis (FALS) with SOD1 H46R mutation in large Japanese families. *Acta Neuropathol.* **2003**, *106*, 561−568.
(20) Holmoy, T.; Bjorgo, K.; Roos, P. M. Slowly progressing amyotrophic lateral sclerosis caused by H46R SOD1 mutation. *Eur. Neurol.* **2007**, *58*, 57−58.
(21) Zou, Z. Y.; Liu, M. S.; Li, X. G.; Cui, L. Y. H46R SOD1 mutation is consistently associated with a relatively benign form of amyotrophic lateral sclerosis with slow progression. *Amyotrophic Lateral Scler. Frontotemporal Degener.* **2016**, *17*, 610−613.
(22) Wang, Q.; Johnson, J. L.; Agar, N. Y.; Agar, J. N. Protein aggregation and protein instability govern familial amyotrophic lateral sclerosis patient survival. *PLoS Biol.* **2008**, *6*, No. e170.
(23) Tu, P. H.; Raju, P.; Robinson, K. A.; Gurney, M. E.; Trojanowski, J. Q.; Lee, V. M. Transgenic mice carrying a human mutant superoxide dismutase transgene develop neuronal cytoskeletal pathology resembling human amyotrophic lateral sclerosis lesions. *Proc. Natl. Acad. Sci. U. S. A.* **1996**, *93*, 3155−3160.
(24) Mayer, S.; Rudiger, S.; Ang, H. C.; Joerger, A. C.; Fersht, A. R. Correlation of levels of folded recombinant p53 in *escherichia coli* with thermodynamic stability in vitro. *J. Mol. Biol.* **2007**, *372*, 268−276.
(25) Okado-Matsumoto, A.; Fridovich, I. Subcellular distribution of superoxide dismutases (SOD) in rat liver: Cu,Zn-SOD in mitochondria. *J. Biol. Chem.* **2001**, *276*, 38388−38393.
(26) Jonsson, P. A.; Graffmo, K. S.; Andersen, P. M.; Brannstrom, T.; Lindberg, M.; Oliveberg, M.; Marklund, S. L. Disulphide-reduced superoxide dismutase-1 in CNS of transgenic amyotrophic lateral sclerosis models. *Brain* **2006**, *129*, 451−464.
(27) Ayers, J. I.; McMahon, B.; Gill, S.; Lelie, H. L.; Fromholt, S.; Brown, H.; Valentine, J. S.; Whitelegge, J. P.; Borchelt, D. R. Relationship between mutant Cu/Zn superoxide dismutase 1 maturation and inclusion formation in cell models. *J. Neurochem.* **2017**, *140*, 140−150.
(28) Roberts, B. R.; Lim, N. K. H.; McAllum, E. J.; Donnelly, P. S.; Hare, D. J.; Doble, P. A.; Turner, B. J.; Price, K. A.; Lim, S. C.; Paterson, B. M.; et al. Oral treatment with Cu(II)(atsm) increases mutant SOD1 in vivo but protects motor neurons and improves the phenotype of a transgenic mouse model of amyotrophic lateral sclerosis. *J. Neurosci.* **2014**, *34* (23), 8021−8031.
(29) Williams, J. R.; Trias, E.; Beilby, P. R.; Lopez, N. I.; Labut, E. M.; Bradford, C. S.; Roberts, B. R.; McAllum, E. J.; Crouch, P. J.; Rhoads, T. W.; Pereira, C.; Son, M.; Elliott, J. L.; Franco, M. C.; Estevez, A. G.; Barbeito, L.; Beckman, J. S. Copper delivery to the CNS by CuATSM effectively treats motor neuron disease in SOD(G93A) mice co-expressing the Copper-Chaperone-for-SOD. *Neurobiol. Dis.* **2016**, *89*, 1−9.
(30) Farrawell, N. E.; Yerbury, M. R.; Plotkin, S. S.; McAlary, L.; Yerbury, J. J. CuATSM protects against the In vitro cytotoxicity of wild-type-like copper-zinc superoxide dismutase mutants but not mutants that disrupt metal binding. *ACS Chem. Neurosci.* **2019**, *10*, 1555−1564.
(31) Capper, M. J.; Wright, G. S. A.; Barbieri, L.; Luchinat, E.; Mercatelli, E.; McAlary, L.; Yerbury, J. J.; O'Neill, P. M.; Antonyuk, S. V.; Banci, L.; et al. The cysteine-reactive small molecule ebselen facilitates effective SOD1 maturation. *Nat. Commun.* **2018**, *9* (1), 1693.
(32) Waldo, G. S.; Standish, B. M.; Berendzen, J.; Terwilliger, T. C. Rapid protein-folding assay using green fluorescent protein. *Nat. Biotechnol.* **1999**, *17*, 691−695.
(33) Tomiyama, T.; Nagata, T.; Shimada, H.; Teraoka, R.; Fukushima, A.; Kanemitsu, H.; Takuma, H.; Kuwano, R.; Imagawa, M.; Ataka, S.; Wada, Y.; Yoshioka, E.; Nishizaki, T.; Watanabe, Y.; Mori, H. A new amyloid beta variant favoring oligomerization in Alzheimer's-type dementia. *Ann. Neurol.* **2008**, *63*, 377−387.
(34) Viola, K. L.; Klein, W. L. Amyloid beta oligomers in Alzheimer's disease pathogenesis, treatment, and diagnosis. *Acta Neuropathol.* **2015**, *129*, 183−206.
(35) Zetterstrom, P.; Graffmo, K. S.; Andersen, P. M.; Brannstrom, T.; Marklund, S. L. Composition of soluble misfolded superoxide dismutase-1 in murine models of amyotrophic lateral sclerosis. *NeuroMol. Med.* **2013**, *15*, 147−158.
(36) Zhang, F.; Zhu, H. Intracellular conformational alterations of mutant SOD1 and the implications for fALS-associated SOD1 mutant induced motor neuron cell death. *Biochim. Biophys. Acta* **2006**, *1760*, 404−414.
(37) Alnuami, A. A.; Zeedi, B.; Qadri, S. M.; Ashraf, S. S. Oxyradical-induced GFP damage and loss of fluorescence. *Int. J. Biol. Macromol.* **2008**, *43*, 182−186.
(38) Haupts, U.; Maiti, S.; Schwille, P.; Webb, W. W. Dynamics of fluorescence fluctuations in green fluorescent protein observed by fluorescence correlation spectroscopy. *Proc. Natl. Acad. Sci. U. S. A.* **1998**, *95*, 13573−13578.
(39) Culotta, V. C.; Klomp, L. W.; Strain, J.; Casareno, R. L.; Krems, B.; Gitlin, J. D. The copper chaperone for superoxide dismutase. *J. Biol. Chem.* **1997**, *272*, 23469−23472.
(40) Furukawa, Y.; Torres, A. S.; O'Halloran, T. V. Oxygen-induced maturation of SOD1: a key role for disulfide formation by the copper chaperone CCS. *EMBO J.* **2004**, *23*, 2872−2881.
(41) Southon, A.; Szostak, K.; Acevedo, K. M.; Dent, K. A.; Volitakis, I.; Belaidi, A. A.; Barnham, K. J.; Crouch, P. J.; Ayton, S.; Donnelly, P. S.; Bush, A. I. Cu(II) (atsm) inhibits ferroptosis: Implications for treatment of neurodegenerative disease. *Br. J. Pharmacol.* **2020**, *177*, 656−667.
(42) Masaldan, S.; Bush, A. I.; Devos, D.; Rolland, A. S.; Moreau, C. Striking while the iron is hot: Iron metabolism and ferroptosis in neurodegeneration. *Free Radical Biol. Med.* **2019**, *133*, 221−233.
(43) Satoh, T.; Ishige, K.; Sagara, Y. Protective effects on neuronal cells of mouse afforded by ebselen against oxidative stress at multiple steps. *Neurosci. Lett.* **2004**, *371*, 1−5.
(44) Stevens, J. C.; Chia, R.; Hendriks, W. T.; Bros-Facer, V.; van Minnen, J.; Martin, J. E.; Jackson, G. S.; Greensmith, L.; Schiavo, G.; Fisher, E. M. Modification of superoxide dismutase 1 (SOD1) properties by a GFP tag−implications for research into amyotrophic lateral sclerosis (ALS). *PLoS One* **2010**, *5*, No. e9541.
(45) Tanaka, N.; Kimura, S.; Kamatari, Y. O.; Nakata, K.; Kobatake, Y.; Inden, M.; Yamato, O.; Urushitani, M.; Maeda, S.; Kamishina, H. In vitro evidence of propagation of superoxide dismutase-1 protein aggregation in canine degenerative myelopathy. *Vet. J.* **2021**, *274*, 105710.

https://doi.org/10.1021/acschemneuro.5c00668
ACS Chem. Neurosci. 2026, 17, 1469−1478